CHARACTERISTICS OF MESOSPHERIC INTERNAL GRAVITY WAVES OBSERVED BY MU RADAR

Y. Muraoka[1], K. Kawahira[2], T. Sato[3], T. Tsuda[3], S. Fukao[3] and S. Kato[3]

Abstract. We present mesospheric wind data from MU radar at Shigaraki (34.9°N, 136.1°E), Japan, that exhibit a wave motion with a vertical wavelength of 6 km. An analysis of the horizontal and vertical components of the observed wind velocity shows that the wave motion is due to an internal inertia-gravity wave. It behaves like a stationary wave, similar to lee waves. With the estimated wave parameters, we can derive the mean mesospheric temperature from the dispersion relation for the inertial modes. The temperature is shown to be quite consistent with the mean state of the atmosphere. It is further shown that a scattering echo layer observed simultaneously was closely connected with the vertical propagation of the gravity waves.

Introduction

In recent years, it has been demonstrated that gravity waves play a significant role in the dynamics of the middle atmosphere [cf. Fritts, 1984]. The vertically propagating modes can transport momentum and energy upwards, and their amplitudes grow exponentially, but less rapidly than $e^{z/2H}$ in the middle atmosphere [Hines, 1960]. Theoretical studies have further shown that the observed circulation and mean temperature structure in the middle atmosphere are maintained through the dissipation and wave drag process of these waves in the mesosphere [Lindzen, 1981; Matsuno, 1982; Holton, 1982, 1983]. The dissipation of gravity waves and the resultant generation of turbulence are considered to be due to dynamical and convective instabilities [Hodges, 1967; Hines, 1970; Lindzen, 1981; Fritts and Dunkerton, 1984; Fritts and Rastogi, 1985].

However, we are only just beginning to fully understand various aspects of gravity wave propagation through a number of observational studies [cf. Fritts et al., 1984a]. Several studies have shown that gravity waves have a wide variety of periods, phase speeds, and horizontal and vertical wavelengths [Vincent and Reid, 1983; Meek et al., 1985]. Little is known about the behavior of mesospheric inertial modes affected by the earth's rotation although some workers have examined this question observationally in the stratosphere by using rocket sounding data [Hirota, 1984; Hirota and Niki, 1985] and in the mesosphere by using VHF echo data [Balsley et al., 1983; Fritts et al., 1984b].

In numerous observational techniques, MU (middle and upper atmosphere) radar is potentially very helpful for studying large- and small-scale motions in the middle atmosphere [Kato et al., 1984; Fukao et al., 1985a, b]. The radar can provide reasonably high spatial and temporal resolution data on atmospheric motions and turbulent intensities [e.g., Sato et al., 1985; Tsuda et al., 1985]. One of the advantages of MU radar measurements is that the vertical wind velocity can be estimated, as well as the horizontal velocity. This permits further detailed discussion of the propagation of gravity waves.

The purpose of this paper is to discuss the characteristics of internal inertia-gravity waves in the mesosphere, by comparing changes in three components of the mesospheric wind field measured by MU radar with the result derived from a simplified linear theory. In addition, we discuss the association between the vertical propagation of the inertial modes and the occurrence of a scattering echo layer in the mesosphere.

MU Radar Observations

The MU radar at Shigaraki (34.9°N, 136.1°E), Japan, is now in full operation with all 475 yagis and 1 MW peak power. Details of the system and experimental results may be found in Kato et al. [1984], Fukao et al. [1985a, b] and Sato et al. [1985]. To measure three components of the wind velocity in the mesosphere, the main beam of the MU radar was pointed vertically and in two off-vertical directions (10° from the zenith), in turns. The main parameters of the MU radar on our observation on September 20, 1985, are listed in Table 1. Echo signals were sampled at intervals of 600 m in the height range of 60-97.8 km and were coherently integrated over 20 pulses of transmission. The signals were transformed into power spectra by using the 128-point FFT. After we removed the effect of meteor echoes observed intermittently above 85 km (see Tsuda et al. [1985] for the behavior of meteor echoes), we determined the radial wind velocities, using a nonlinear least square fitting method for the Doppler shifted spectrum data that were incoherently accumulated for about 30 min. The meridional and zonal components of the mesospheric wind velocity were derived from the radial velocities considering the vertical component. The average of the four successive wind profiles was estimated as a mean profile for about two hours and was smoothed by applying a three-point running mean to remove small-scale noise. Furthermore, the contribution of large-scale components with vertical scales larger than about 20 km, which are due to the background mean flow, tides and so on, was estimated by applying a low-pass filter with respect to height.

Results

Figure 1 shows a time-height contour of the echo intensity scattered at mesospheric heights in the vertical direction of the beam during 1145-1645 LT on September 20, 1985. Between 65 and 85 km in altitude, three intense echo layers were

[1] Department of Physics, Hyogo College of Medicine
[2] Geophysical Institute, Kyoto University
[3] Radio Atmospheric Science Center, Kyoto University

Paper number 7L6574.
0094-8276/87/007L-6574$03.00

TABLE 1. Parameters of the mesospheric measurements by MU radar.

Height range	60 - 97.8 km
Beam frequency	46.5 MHz
Beam directions	vertical northward deflected 10° from the zenith eastward deflected 10° from the zenith
Sample intervals	600 m
Time resolution	208 sec
Inter-pulse period	1300 μsec

observed continually around the heights of 70, 76 and 82 km. During the observation, the heights of these layers changed very little, while the intensity decreased. The change in echo intensity may be divided into two periods, since the intensity became weak once around 1400 LT. Thus, we estimated two mean wind profiles from these scattering echo data. Figure 1 also shows that meteor echoes were observed intermittently above 85 km.

Figure 2 shows the height profiles of the mean wind velocity for the zonal, meridional and vertical components between 60 and 90 km in the latter half of the period during which intense echo layers were observed (1431-1635 LT). This figure indicates that a wave motion with a vertical wavelength of 6 km existed in the background mean flow. The amplitude of the velocity perturbation increased with height up to 80 km, as typically occurs in the meridional component. The magnitudes attained 11 m/s, 17 m/s and 25 cm/s in the zonal, meridional and vertical components, respectively, near 80 km height. At the same time, the background mean flow had eastward and northward components on the order of 20 m/s with downward motion of approximately 20 cm/s, although they varied gradually with height. Note that the northward and downward components of the wind velocity perturbation due to the wave motion were well correlated with each other. They were apparently connected with the appearance of the echo layers shown in Figure 1, with a constant phase phase difference (~π/3). It is noted that the echo layers also corresponded to the strong vertical shear of the zonal wind. Figure 3 is another example of the mean wind profiles, which were estimated from the earlier half (1202-1407 LT) of the echo data shown in Figure 1. This figure also shows the existence of a wave motion with a vertical wavelength of 6 km although it was disturbed by small-scale noise. The perturbation winds due to the wave correspond to the simultaneously observed echo layers, as in Figure 2.

Discussion

We proceed now to estimate various parameters of the observed wave motion, with a simplified theory for inertial gravity waves [e.g., Gossard and Hooke, 1975]. We assume that the perturbations in the linearized equations have solutions proportional to $\exp\{i(kx+mz-\omega t)\}$. Here k and m are the horizontal and vertical wave numbers, and ω is the observed (Doppler-shifted) frequency. Considering a background mean flow, $\bar{u}$ in the x direction, the intrinsic frequency with respect to the mean flow is defined as

$$\hat{\omega} \equiv \omega - k\bar{u}. \quad (1)$$

To a good approximation, a dispersion relation for inertial gravity waves ($N > \hat{\omega} \geq f$),

$$m^2 = \frac{k^2N^2}{\hat{\omega}^2 - f^2} \quad (2)$$

is obtained. Here f is the inertial frequency and N is the Brunt-Väisälä frequency. Then, the polarization relations between perturbation velocity components are given by

$$v' = -(if/\hat{\omega})\,u' \quad (3)$$

and

$$w' = -(k/m)\,u'. \quad (4)$$

We consider the wave motion shown in Figure 2 here because the estimated wave parameters are almost the same as those in Figure 3 except for a slight difference in the direction of horizontal propagation. In Figure 4, the change in wind velocity with height is shown for the zonal-

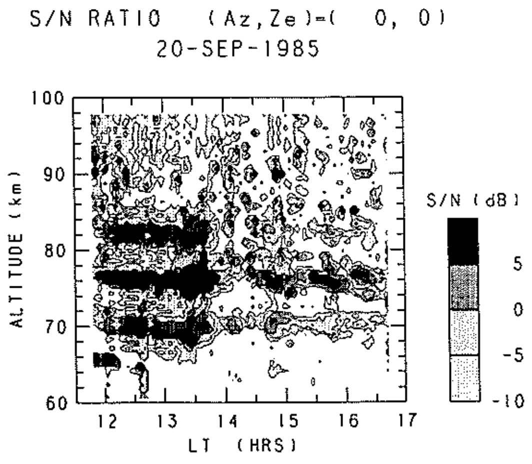

Fig. 1. Time-height contour of signal-to-noise (S/N) ratio observed in the vertical beam direction of the MU radar on September 20, 1985. The S/N ratio is defined in an arbitary unit.

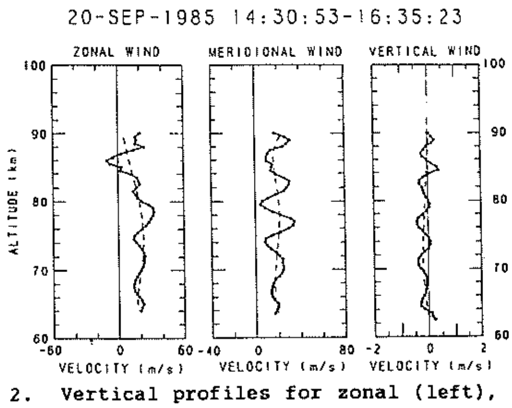

Fig. 2. Vertical profiles for zonal (left), meridional (center) and vertical (right) components of mean mesospheric wind velocity observed by the MU radar between 1431 and 1635 LT on September 20, 1985. Each positive value indicates eastward, northward and upward winds, respectively. Dashed line in each panel represents the background mean flow smoothed by a low-pass filter.

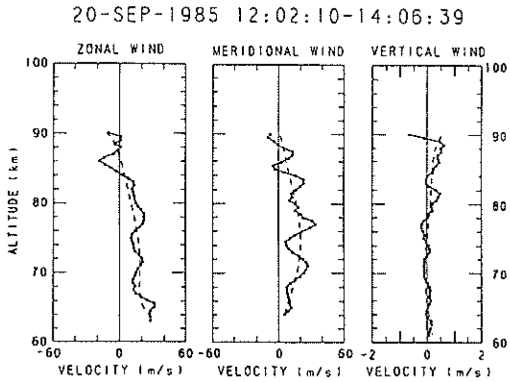

Fig. 3. Same as Figure 2 except for observation between 1202 and 1407 LT on the same day.

meridional and meridional-vertical components of the wind profiles shown in Figure 2. Figure 4(a) clearly shows that the direction of the horizontal perturbation wind rotates clockwise with increasing height. Figure 4(b) shows that the downward perturbation wind has a good correlation with the northward one. From the polarization relations (3) and (4), the observed wave is shown to propagate almost southward in the horizontal direction and vertically downward (m<0). Taking the x axis in the southward direction, we see further from (4) that the horizontal wavelength ($\lambda_h=2\pi/k$) turns out to be 400 km with the vertical wavelength ($\lambda_z=2\pi/m$) of 6 km and with $w'/u' \sim 0.015$ estimated from Figure 4(b).

The heights of the intense echo layers shown in Figure 1 scarcely changed during our observation and correspond to a phase of the wave motion observed simultaneously. Thus, we can interpret the wave motion as due to a stationary wave similar to lee waves ($\omega \sim 0$). Then, we estimate from (1) that the intrinsic frequency of the wave motion,

$$\hat{\omega} \doteqdot -k\bar{u} = -2\pi\bar{u}/\lambda_h \sim 3.1\times10^{-4}\ s^{-1} \qquad (5)$$

and the period,

$$T = 2\pi/\hat{\omega} = -\lambda_h/\bar{u} \sim 5.6\ h \qquad (6)$$

with $\bar{u} \sim -20$ m/s near 75 km from Figure 2. Thus, we see that $f/\hat{\omega} \sim 0.27$ with $f = 8.3\times10^{-5}\ s^{-1}$ at 34.9°N. This ratio is smaller than the 0.35 estimated directly from the elliptic polarization of the horizontal perturbation wind near 75 km in Figure 4(a). This difference seems to be due to the change in the polarization above 77 km.

Taking account of $(f/\hat{\omega})^2 \ll 1$ in the dispersion relation (2), we find that the Brunt-Väisälä frequency in the mesosphere was

$$N \doteqdot m\hat{\omega}/k = -2\pi\bar{u}/\lambda_z \sim 0.021\ s^{-1} \qquad (7)$$

with the values of $\bar{u}$ and λ_z near 75 km, which were obtained immediately from Figure 2. Thus, the observed wave motion is shown to be due to an inertial gravity wave ($N \gg \hat{\omega} \gtrsim f$). Furthermore, we see that the scale height H of the mean atmosphere is $H=\kappa g/N^2 \sim 6.2$ km with $\kappa=2/7$ and $g=9.6\ ms^{-2}$ near 75 km and that the mean mesospheric temperature is 210 K. These values agree reasonably well, for example, with those at 75 km in the U.S. Standard Atmosphere, 1976.

With respect to the local Richardson number affected by the gravity wave, it is well known that the maximum Richardson number is achieved at that phase of the wave motion at which the total static stability is maximum [cf. Fritts and Rastogi, 1985]. At the height corresponding to the phase, the downward perturbation wind velocity attains its maximum. At the same time, we see that the meridional component is its northward maximum and the vertical shear of zonal component is its maximum for southward propagation. It is shown from a comparison of Figure 1 with Figures 2 and 3 that the observed echo layers correspond to the regions indicating the downward and northward perturbation wind and the strong vertical shear of the zonal perturbation wind, with a constant phase difference ($\sim\pi/3$). At present, we cannot suggest what dynamical effect produces the phase difference. However, we believe that the echo layers are primarily associated with the statically stabilized regions which are produced by the gravity wave propagation.

Concluding Remarks

We have shown that the observed wave motions satisfy the dispersion relation for inertial gravity waves ($N \gg \hat{\omega} \gtrsim f$). At the same time, it has been shown that we can derive reasonable values for the mean mesospheric scale height and temperature from the wave parameters. This indicates that MU radar is useful not only for measuring the mesospheric wind velocity with sufficient accuracy but also for investigating the behavior of atmospheric gravity waves in the mesosphere.

We have also shown that the observed inertial gravity wave was as stationary as lee waves. This may be an indication of the vertical propagation of topographically forced waves with $\omega = 0$ in the winter hemisphere, as has been suggested by Lindzen [1981] and Holton [1982]. It is noted that the observed wave was stationary in the northward mean flow. This suggests that the wave source was to the south of our station. At the same time, the ratio of $f/\hat{\omega}$ for the wave was around 0.3. This ratio agrees well with that obtained in the upper stratosphere with meteorological rocket data by Hirota and Niki [1985]. Assuming a topographically forced wave ($\omega = 0$ and k = const.), the intrinsic frequency must be proportional to the mean flow velocity. This may be an indication that the

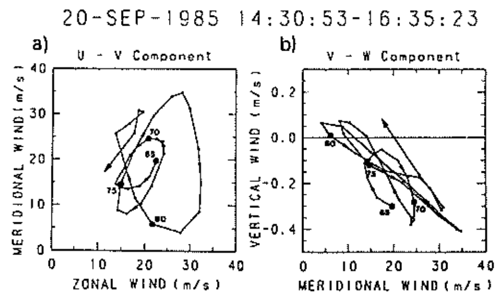

Fig. 4. Hodograph representations of the height change of the mean mesospheric wind velocity shown in Figure 2, in zonal - meridional (a) and meridional-vertical (b) planes. The altitudes at which wind velocity is measured are indicated at every 5 km in height in each panel.

magnitude of the mean flow is limited near the source region of such waves.

We have shown that the observed intense echo layers are connected with the vertical propagation of the inertial gravity wave. These layers correspond to the regions indicating the downward perturbation wind. Thus, there is little doubt that the appearance of intense echo layers is associated with the total static stability in the atmosphere disturbed by the gravity wave motion. However, more detailed analysis is required before a statically stable region can be positively identified with the echo layer in this and many other observations.

Acknowledgments. This study was sponsored by the Radio Atmospheric Science Center, Kyoto University. We thank the staff of Shigaraki MU Observatory for their help with the observations and data analysis. One of the authors (Y. M.) also thanks T. Sato, H. Murata and T. Sugiyama for useful discussions and encouragement.

References

Balsley, B. B., W. L. Ecklund, and D. C. Fritts, VHF echoes from high-latitude mesosphere and lower thermosphere: Observations and interpretations, J. Atmos. Sci., 40, 2451-2466, 1983.

Fritts, D. C., Gravity wave saturation in the middle atmosphere: A review of theory and observations, Rev. Geophys. Space Phys., 22, 275-308, 1984.

Fritts, D. C., and T. J. Dunkerton, A quasi-linear study of gravity-wave saturation and self-acceleration, J.Atmos.Sci.,41, 3272-3289, 1984.

Fritts, D. C., and P. K. Rastogi, Convective and dynamical instabilities due to gravity wave motions in the lower and middle atmosphere: Theory and observations, Radio Sci., 20, 1247-1277, 1985.

Fritts, D. C., M. A. Geller, B. B. Balsley, M. L. Chanin, I. Hirota, J. R. Holton, S. Kato, R. S. Lindzen, M. Schoeberl, R. A. Vincent, and R. F. Woodman, Research status and recommendations from the Alaska Workshop on gravity waves and turbulence in the middle atmosphere, Fairbanks, Alaska, 18-22 July 1983, Bull. Am. Meteorol. Soc., 65, 149-159, 1984a.

Fritts, D. C., B. B. Balsley, and W. L. Ecklund, VHF echoes from the Arctic mesosphere and lower stratosphere, Part II: Interpretations, in Dynamics of the Middle Atmosphere, ed. by J. R. Holton and T. Matsuno, pp.97-115, Terra, Tokyo, 1984b.

Fukao, S., T. Sato, T. Tsuda, S. Kato, K. Wakasugi and T. Makihira, The MU radar with an active phased array system, 1. Antenna and power amplifiers, Radio Sci., 20, 1155-1168, 1985a.

Fukao, S., T. Tsuda, T. Sato, S. Kato, K. Wakasugi, and T. Makihira, The MU radar with an active phased array system, 2. In-house equipment, Radio Sci., 20, 1169-1176, 1985b.

Gossard, E. E., and W. H. Hooke, Waves in the Atmosphere, 456 pp., Elsevier, New York, 1975.

Hines, C. O., Internal gravity waves at ionospheric heights, Can. J. Phys., 38, 1441-1481, 1960.

Hines, C. O., Eddy diffusion coefficients due to instabilities in internal gravity waves, J. Geophys. Res., 75, 3937-3939, 1970.

Hirota, I., Climatology of gravity waves in the middle atmosphere, J. Atmos. Terr. Phys., 46, 767-773, 1984.

Hirota, I., and T. Niki, A statistical study of inertia-gravity waves in the middle atmosphere, J. Meteor. Soc. Japan, 63, 1055-1066, 1985.

Hodges, R. R., Jr., Generation of turbulence in the upper atmosphere by internal gravity waves, J. Geophys. Res., 72, 3455-3458, 1967.

Holton, J. R., The role of gravity wave induced drag and diffusion in the momentum budget of the mesosphere, J.Atmos.Sci.,39, 791-799, 1982.

Holton, J. R., The influence of gravity wave breaking on the general circulation of the middle atmosphere, J. Atmos. Sci., 40, 2497-2507, 1983.

Kato, S., T. Ogawa, T. Tsuda, T. Sato, I. Kimura, and S. Fukao, The middle and upper atmosphere radar: First results using a partial system, Radio Sci., 19, 1475-1484, 1984.

Lindzen, R. S., Turbulence and stress owing to gravity wave and tidal breakdown, J. Geophys. Res., 86, 9707-9714, 1981.

Matsuno, T., A quasi one-dimensional model of the middle atmosphere circulation interacting with internal gravity waves, J. Meteor. Soc. Japan, 60, 215-226, 1982.

Meek, C. E., I. M. Reid, and A. H. Manson, Observations of mesospheric wind velocities. 1. Gravity wave horizontal scales and phase velocities determined from spaced wind observations, Radio Sci., 20, 1363-1382, 1985.

Sato, T., T. Tsuda, S. Kato, S. Morimoto, S. Fukao, and I. Kimura, High-resolution MST observations of turbulence by using the MU radar, Radio Sci., 20, 1452-1460, 1985.

Tsuda, T., M. Yamamoto, T. Sato, and S. Kato, Comparison observations between the MU radar and the Kyoto meteor radar, Radio Sci., 20, 1241-1246, 1985.

Vincent, R. A., and I. M. Reid, HF Doppler measurements of mesospheric gravity wave momentum fluxes, J. Atmos. Sci., 40, 1321-1333, 1983.

S. Fukao, S. Kato, T. Sato, and T. Tsuda, Radio Atmospheric Science Center, Kyoto University, Uji, Kyoto 611, Japan.

K. Kawahira, Geophysical Institute, Kyoto University, Kyoto 606, Japan.

Y. Muraoka, Department of Physics, Hyogo College of Medicine, Nishinomiya 663, Japan.

(Received April 20, 1987;
revised July 13, 1987;
accepted September 7, 1987.)